Ring rotational speed trend analysis by FEM approach in a Ring Rolling process

G.Allegri[1, a)] L.Giorleo[1,b)] E.Ceretti [1,c)]

[1]*Department of Mechanical and Industrial Engineering - University of Brescia – via Branze 38 – Brescia – Italy*

a) *g.allegri001@unibs.it*
b) *luca.giorleo@unibs.it*
c) *elisabetta.ceretti@unibs.it*

Abstract. Ring Rolling is an advanced local incremental forming technology to fabricate directly precise seamless ring-shape parts with various dimensions and materials. In this process two different deformations occur in order to reduce the width and the height of a preform hollow ring; as results a diameter expansion is obtained. In order to guarantee a uniform deformation, the preform is forced toward the Driver Roll whose aim is to transmit the rotation to the ring. The ring rotational speed selection is fundamental because the higher is the speed the higher will be the axial symmetry of the deformation process. However, it is important to underline that the rotational speed will affect not only the final ring geometry but also the loads and energy needed to produce it. Despite this importance in industrial environment, usually, a constant value for the Driver Roll angular velocity is set so to result in a decreasing trend law for the ring rotational speed. The main risk due to this approach is not fulfilling the axial symmetric constrain (due to the diameter expansion) and to generate a high localized ring section deformation. In order to improve the knowledge about this topic in the present paper three different ring rotational speed trends (constant, linearly increasing and linearly decreasing) were investigated by FEM approach. Results were compared in terms of geometrical and dimensional analysis, loads and energies required.

Keywords: *Ring Rolling, Driver Roll angular velocity, FEM*

1.INTRODUCTION

In Ring Rolling process the metal is rolled between two couple of rolls: two radial and two axial. In each couple, one roll moves toward the other, to reduce ring cross section; during the process due to the volume compensation diameter expansion occurs [1,2]. This process is used for the production of railway wheels, anti-friction bearings and different ring shaped workpieces used for automotive, aerospace and wind industry applications. It can be both a hot or cold process [3, 4, 5] and different alloys as steels, aluminum and titanium can be worked [6]. The advantages of Ring Rolling process include: short production time, uniform quality, close tolerances and considerable saving in material cost. The main advantage of the Ring Rolling product, compared to others processes, is given by the size and orientation of the grains. Fig. 1a summarizes the Ring Rolling process: the Idle Roll forces a hollow circular preform against a Driver Roll on the Y direction. At the same time, the Axial rolls apply a pressure in Z direction in order to reduce the height of the ring. A backward movement on the Y-axis is given to the Axial Rolls according to the diameter expansion. Because the ring does not rotate on its own axis, two Guide Rolls are designed to assure the stability of the process.
The displacement of each roll can be set independently from the others. For this reason, in industrial practice the milling curve is introduced as a function of the instantaneous ring height (H) and width (W) (Fig. 1b).

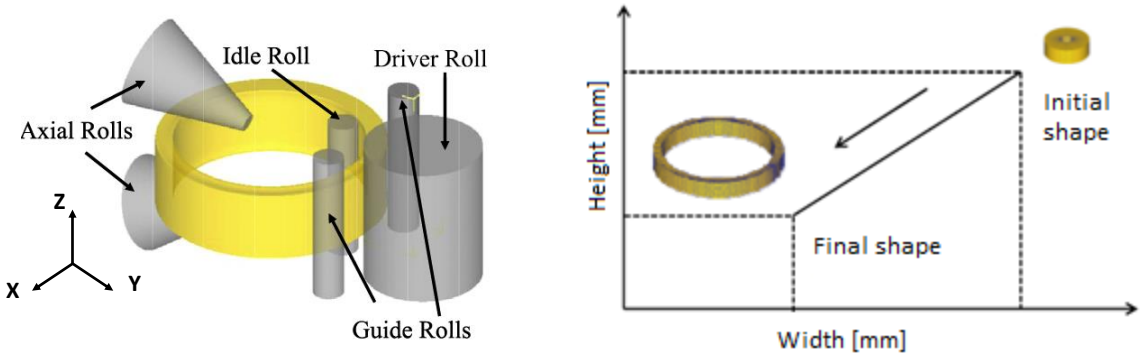

Figure 1.a) Ring Rolling scheme; b) Milling curve for a Ring Rolling process

The milling curve definition is fundamental to guarantee a correct ring production [7, 8]. Usually in the industrial environment, it is common to set constant Driver Roll's angular speed. This means that the angular velocity of the ring decreases as a function of the growth of the external diameter; this can lead to general deformation problems in terms of ring roundness, concentricity and fishtail (the depression of the height along the width measured between the mandrel and the Driver Roll) [9], moreover local deformations of the ring that produce errors on the external diameter (D_{ext}), height (H) and width (W) too. This is due to the non-axial deformation of the ring that increases at decreasing of the ring angular velocity. In literature, there are limited works about the influence of the Driver Roll on the process [10, 11] in which the aim was to study the inhomogeneity distribution of strain, temperature, fishtail coefficient and rolling force parameters. The goal of the present paper was to impose 3 different Driver Roll's rotation laws to study, under a FEM approach, the final geometry of the ring and the forces and energies acting on the milling plant in order to identify which law generates a process better under control. Starting from an industrial case study, an analysis about the benefits to control the angular rotation on the ring has been studied in a previous work [12], applying different constant angular velocities with the goal of verify which constant angular velocity leads to better geometrical parameters of the final product coupled with forces, energies and power required by the milling plant. Based on this consideration in the present paper the authors test the effect of different ring rotational speed laws on the process performance. Results were compared in terms of geometrical and dimensional analysis, loads and energies required.

2.MATERIALS AND METHODS

In this work Deform 3D FEM software was used due to investigate the influence of different non-constant Driver Roll rotation laws. The aim of this paper was to impose 3 different angular velocities of the ring in order to test the difference between a linearly increasing ring rotation (IC) a linearly decreasing ring rotation (DC) and a constant ring rotation (CC) (Fig. 2a) The CC configuration was designed starting from an industrial case study following the assumption reported in [12]. IC has been imposed starting from a reduction of 50% on CC and reaching, at the end of the milling, a rotational angular velocity increased of 50%; on the other hand, DC starts from an angular velocity of the ring that is 50% higher than CC and it's reduced of 50% at the end of the milling process. Figure 2b shows the Idle and Axial roll laws imposed.

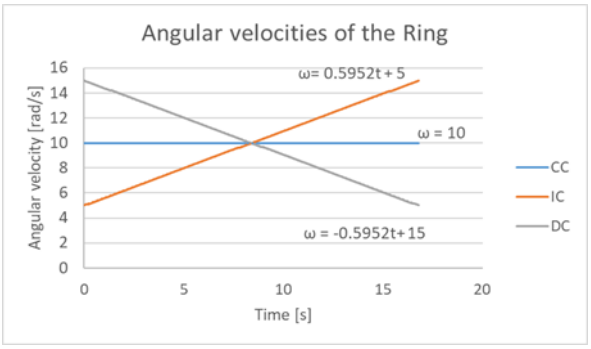

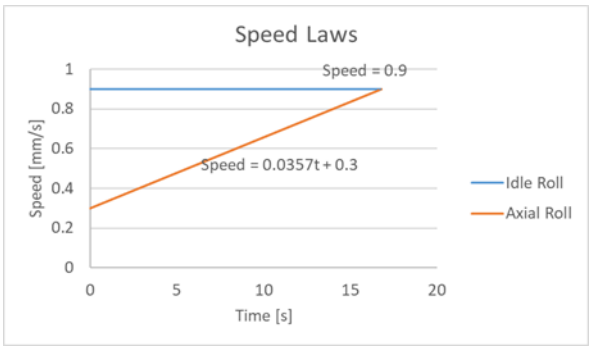

a) b)

Figure 2. a) Angular velocities of the Ring; b) Speed laws for Idle and Axial Roll

The main characteristics of ring and milling parameters are summarized in Table 1 and Table 2. Due to the self-centering properties the software allows to simulate the process without the Guide Rolls. The simulation is limited to model half ring considering the symmetry on the XY plane; the rolls were considered as rigid bodies and tetrahedral mesh was used with 10680 elements for the workpiece. A friction factor of 0.7 was imposed between the rolls and the object and no heat exchange was set because there was not difference between the results in the isothermal simulation and the heat exchange simulation; this is due to the short milling time; in addition, a constant ring temperature can be detected during the actual process. AISI 1045 was chosen from DEFORM library.

Table 1: Ring dimensions

Ring	**H [mm]**	**W [mm]**	**Dext [mm]**
Preform	75	69	258
Finished Ring	56	50	373

Table 2: Milling parameters

Material	AISI 1045
Workpiece Temperature °C	1150
Milling time [s]	16.8
Idle Roll Diameter [mm]	110
Driver Roll Diameter [mm]	700
Driver Roll angular velocity [rad/sec]	F(t)
Axial Roll Height [mm]	400
Axial Roll taper angle [°]	15.7
Idle Roll speed [mm/s]	0.9
Axial Roll speed [mm/s]	H(t))/t

Starting from the Idle Roll and Axial Roll's speed laws and imposing the constant volume constrain, the diameter expansion of the ring was evaluated (Equation 2) using an analytical model (AM). The Driver roll angular velocity rotation equation has been derived imposing that the peripheral velocity at the contact point between the Driver Roll and the ring is the same, Equation 2 has been used for calculating the law of the Driver Roll as function of time.

$$\emptyset 1(t) = \frac{1}{W(t)} \cdot \left(\frac{V}{\pi \cdot H(t)} + W(t)^2\right) \quad (1)$$

$$\omega 2(t) = \emptyset 1(t) \cdot \omega 1(t)/\emptyset 2 \quad (2)$$

Being:
$\emptyset 1(t)$=External diameter of the ring;
$\emptyset 2$=Diameter of the Driver Roll;
$\omega 1(t)$=Angular velocity of the ring;
$\omega 2(t)$=Angular velocity of the Driver Roll;
W(t)=Width reduction of the ring as function of time;
V=Volume of the ring;
$H(t)$=Height reduction of the ring as function of time.
Table 3 resumes the imposed angular velocities for the ring and the consequent angular velocity of Driver Roll.

Table 3: Details of the simulations performed

Test	**Ring Angular Velocity Rad/s ($\omega 1$)**	**Driver Roll Angular Velocity Rad/s ($\omega 2$)**
CC	10	$0.0002t^3 + 0.0006t^2 + 0.05t + 3.6078$
IC	$0.5952t + 5$	$0.0005t^3 - 0.0003t^2 + 0.2531t + 1.7930$
DC	$-0.5952t + 15$	$-0.0001t^3 + 0.0016t^2 - 0.153t + 5.4227$

All the output parameters have been measured using Deform 3D post process software and GOM Inspect software. Regarding the geometrical parameters, the external diameter, the height, the width, the fishtail, the external and internal roundness and the concentricity of the ring, have been evaluated following this method:

- External Diameter (Dext): using a point tracking command, picking two points at 180°. This operation has been performed three times along the height of the ring in order to check its deviation (Fig.3a P1-P2, P3-P4, P5-P6).
- Height (H): using the command "circulary pattern" five circumferences of 200 points have been performed in order to measure the height of the whole ring (Fig.3b H1-H5).
- Width (W): it has been measured 4 times at 90° along the ring [Fig.3b] (W1-W4).
- Fishtail: using a Following boundary of 200 points the height of the ring has been measured in the section between the Driver Roll and the mandrel (F) (Fig.4a).

For the measurement of the external and internal roundness and the circularity of the ring, a CAD model has been aligned with the object in output from DEFORM FEM software and measured using Gom Inspect software (Fig.4b)
For the physical parameters the maximum load and the energy required for the milling process have been extracted. Regarding the Driver Roll the maximum torque and the maximum power have been considered.

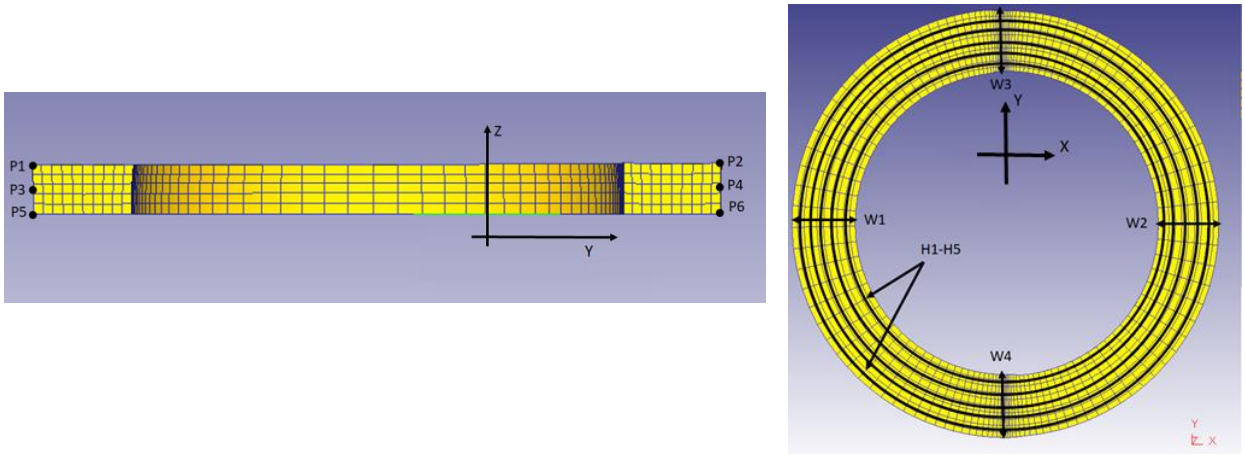

a) b)

Figure 3. a) Measurement of the external diameters; b) Measurement of the heights and widths

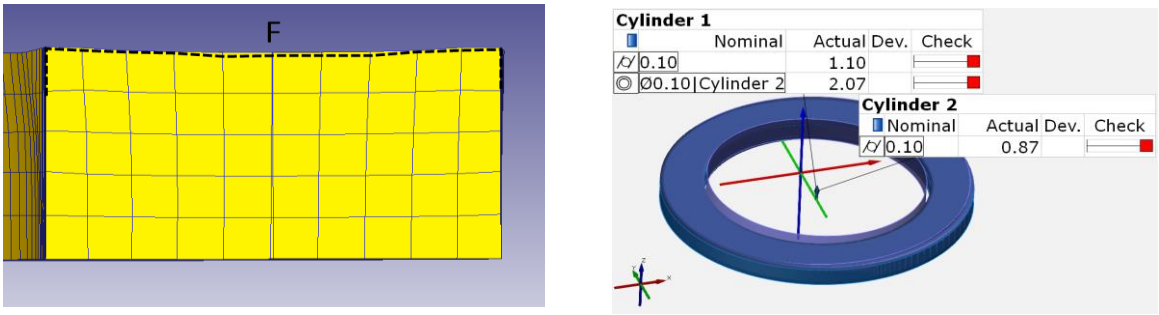

a) b)

Figure 4. a) Measurement of the fishtail; b) Measurement of the external and internal roundness and of the concentricity

3. RESULTS AND DISCUSSIONS

Table 4 shows the geometry of the ring obtained at the end of each simulation and the target on the geometry obtained from equations 1 and 2; in this table the ring geometry evaluated with an analitical model (AM) having no fishtail, roundness and concentricity errors are reported too. Table 5 reports the physical parameters.

Table 4: Geometrical results

Test	D_{ext} [mm]	σ_{Dext}	H [mm]	σ_H	W [mm]	σ_w	Fishtail [mm]	External roundness [mm]	Internal roundness [mm]	Concentricity [mm]
CC	380.34	0.499	27.65	0.327	55.02	1.359	0.74	1.1	0.87	2.07
IC	382.32	0.413	27.50	0.198	54.64	0.947	0.69	0.66	0.66	1.40
DC	373.51	0.725	27.99	0.545	55.74	2.109	1.15	1.68	1.68	4.60
AM	387.39		27.25		53.80					

Results show that IC has an external diameter, height and width closer to the analytical model (AM) and lower standard deviation compared to the others two cases. The fishtail defect is lower in the IC simulation compared to CC and DC. Also in these three measurements, IC presents a better geometry compared with the other two cases. The reduction of the standard deviation on the IC model means that the process is more in control and this leads to a better properties and cost reduction.

Table 5: Physical results

Test	Idle_F_{MAX} [N]	Idle_Energy [J]	Axial_ F_{MAX} [N]	Axial_Energy [J]	Torque [Nm]	Power [W]
CC	8.19E+04	6.71E+02	1.37E+06	1.37E+03	6.75E+03	3.39E+04
IC	9.02E+04	6.61E+02	1.35E+06	1.35E+03	7.46E+03	3.82E+04
DC	8.29E+04	6.07E+02	1.37E+06	1.37E+03	7.62E+03	2.81E+04

Regarding the physical parameters IC has higher values on the maximum load measured on the Idle Roll. The Idle Energy, the Axial maximum Load and the Axial Energy are comparable. Considering the torque, DC (that is the configuration that produces the ring with worse geometry compared with the other two simulations) presents the lowest value; the comparison between CC and IC shows that IC presents a torque higher and this is due to the higher angular velocity imposed. The maximum power is almost the same for CC and IC configuration while DC presents a lower consumption.

4. CONCLUSIONS

The aim of this work was to investigate the influence of different Driver Roll's rotation laws on the Ring Rolling process. Three different angular velocities of the ring have been investigated: linearly increasing (IC), constant (CC) and linearly decreasing (DC). The Driver Roll speed laws used in order to guarantee these angular velocities were derived using an analytical model starting from the milling curve equation coupled with the constant volume constrain. The paper highlights that DC, that is the configuration more similar to the one used in the industrial environment, is the configuration that results in a poor quality in terms of the geometry of the ring. Imposing the IC configuration means that at the beginning of the process the ring rotates at lower velocity and there is an inhomogeneous deformation due to the asymmetry of the milling process; however, the increasing of the rotational speed of the ring leads to fulfill the lack of the geometrical quality obtained during the initial step. Results show that IC configuration is better than CC in terms of geometrical results on the ring guarantying a process more in control. Considering the physical parameters acting on the milling plant, the small difference in terms of maximum torque and power required by the milling plant between CC and IC configuration confirms that IC is a good solution to produce a high quality ring. Further simulations are ongoing in order to find the optimum ring rotational speed to test in the industrial environment.

REFERENCES

1. E. Eruc, R. Shivpuri, International Journal of Machine Tools and Manufacturing **32**, 379–98 (1992).
2. J. Allwood, A. Tekkaya, T. Stanistreet, Steel Research International, **76**, 111–20 (2005).
3. L. Guo, H. Yang, M. Zhan, Modeling and Simulation in Material Science and Engineering, **13**, 1029-1046 (2005).
4. F. Yan, L. Hua, Y. Wu, International Journal of Machine Tools and Manufacturing, **47**, 1695-1701 (2007).
5. Z. Lu, J. Wu, R. Guo, R, L. Xu, R.Yang, Acta Metallurgica Sinica, **30**, 621-629 (2017).
6. S. Yu, C. Liu, Y. Gao, S. Jiang, Z. Bao, Materials Characterization, **131**, 135-139 (2017).
7. L. Giorleo, E. Ceretti, C. Giardini, Key Engineering Materials, **651**, 248-253 (2015).
8. L. Giorleo, E. Ceretti, C. Giardini, Key Engineering Materials, **622**, 956-963 (2014).
9. L. Giorleo, E. Ceretti, C. Giardini, Transactions of the North American Manufacturing Research Institution of SME, **40**, 104-111 (2012).
10. L. Xiao, L. Lian, X. Wen, Z. Yong, Journal of Magnesium and alloys, **2**, 2213-9567 (2014).
11. L. Xiao, L. Lian, X. Wen, Z. Yong, Advanced Materials Research, **773**, 309-315 (2015).
12. G. Allegri, L. Giorleo, E. Ceretti, C. Giardini, Procedia Engineering, **207**, 1230-1235 (2017).